



# Spectral, optical, and cytotoxicity studies on *N*-(2-isonicotinoylhydrazine-carbonothioyl)benzamide and its metal complexes

Nasser Mohammed Hosny<sup>1</sup> | Heba M. Mahmoud<sup>1</sup> | Mohamed H. Abdel-Rhman<sup>2</sup>

<sup>1</sup>Chemistry Department, Faculty of Science, Port-Said University, Port-Said, Egypt

<sup>2</sup>Chemistry Department, Faculty of Science, Mansoura University, Mansoura, Egypt

## Correspondence

Nasser Mohammed Hosny, Chemistry Department, Faculty of Science, Port-Said University, Port-Said, Egypt.

Email: Nasserh56@yahoo.com

and

Mohamed H. Abdel-Rhman, Chemistry Department, Faculty of Science, Mansoura University, Mansoura, Egypt.

Email: mhassan2371@yahoo.com

## Abstract

The ligand *N*-(2-isonicotinoylhydrazine-carbonothioyl)benzamide ( $H_3L$ ) and its metal complexes with Co(II), Ni(II), Cu(II), and Zn(II) acetates have been synthesized. The synthesized compounds have been characterized by elemental analyses, FT-IR, UV-Visible spectra, <sup>1</sup>H-NMR, <sup>13</sup>C-NMR, ESR, MS, effective magnetic moments, molar conductance, and thermal analyses. The free organic ligand exists in the keto form, but in the metal complexes, it forms chelates with the metal ions in the enol form. The measured optical band gap ( $E_g$ ) values confirmed the presence of direct electronic transition and the semiconductivity of the current compounds. The ligand and its Zn(II) complex were examined as cytotoxic agents against HePG-2 and HCT-116 and showed.  $H_3L$  exhibited strong cytotoxicity, while Zn complex showed moderate activity.

## 1 | INTRODUCTION

To face the increasing challenge of antimicrobial drug-resistant microorganisms, many researches are performed to design and synthesize new compounds with potent therapeutic activity.<sup>[1]</sup> Isoniazid has attracted much more attention due to its anti-tuberculostatic, anti-bacterial, and anti-depressant properties. These properties have attracted further research on isoniazid and its derivatives.<sup>[2]</sup>

Thiosemicarbazides are among the most interesting compounds in biological chemistry due to their high activities as biocidal, antifungal, antibacterial, anticonvulsant,<sup>[3-6]</sup> and antitumor.<sup>[7,8]</sup> Also, thiosemicarbazides could be considered important class in different branches of chemistry. It is used as analytical agents for the analysis of different metal ions.<sup>[9]</sup>

It was found that the antitumor activity of some thiosemicarbazides increases by coordinating to certain metal ions.<sup>[10]</sup> To obtain efficient chemotherapeutic agents, much more effort has been direct to modify structure and to the interpretation of the structure-activity relationships. For example, in the pyridyl derivatives of thiosemicarbazide, it was found

that, replacement of the sulfur atom of the thiocarbonyl group by oxygen leads to decreasing the activity whereas, selenium maintains the activity. Also, the position of the attached substituents to the pyridyl ring is very effective factor in determining the antitumor activity.<sup>[11]</sup>

The main transition metal ions as cobalt, nickel, and copper are essential for both animals and plants. They incorporate as cofactor in many oxidative enzymes and vitamins as lactase, hydrogenase, tyrosinase, vitamin B<sub>12</sub>, and cytochrome oxidase.<sup>[12]</sup>

The phenyl, *p*-methylphenyl, *p*-methoxyphenyl, and *p*-chlorophenyl isothiocyanate derivatives of isonicotinic acid hydrazide were synthesized and characterized.<sup>[13,14]</sup> On continuation to our previous efforts on the metal complexes of isonicotinic thiosemicarbazide derivatives, ethyl, and benzoyl thiosemicarbazide derivatives have been reported.<sup>[15,16]</sup>

This work aims to synthesize and characterize a new ligand *N*-(2-isonicotinoylhydrazine-carbonothioyl)benzamide and its complexes with some divalent metal ions. To shed light on the possible activity of the present compounds the cytotoxicity activity of these compounds has been investigated.

## 2 | RESULTS AND DISCUSSION

The elemental analyses and some physical properties of the isolated ligand and its metal complexes are presented in Table 1. The results indicated that the isolated complexes have (1:1) (M:L) stoichiometry. They have high melting point (>300°C) and insoluble in most common organic solvents but soluble in DMF and DMSO. The molar conductance values of all complexes are in the range 5.0-9.0  $\Omega^{-1} \text{ cm}^2 \text{ mol}^{-1}$  indicating their non-electrolytic nature.

### 2.1 | IR spectra

The infrared spectra of  $\text{H}_3\text{L}$ , as KBr disk, showed sharp band at  $3211 \text{ cm}^{-1}$  with shoulders at  $3243$  and  $3147 \text{ cm}^{-1}$  assigned to  $\nu(\text{N}^2\text{H})$ ,  $\nu(\text{N}^4\text{H})$ , and  $\nu(\text{N}^1\text{H})$  vibrations,<sup>[16]</sup> respectively. Moreover, three sharp bands appear at  $1691$ ,  $1672$ , and  $1640 \text{ cm}^{-1}$  attributed to  $\nu(\text{C}=\text{O})_{\text{Ph}}$ ,<sup>[17-19]</sup>  $\nu(\text{C}=\text{O})_{\text{Py}}$ ,<sup>[16]</sup> and  $\nu(\text{C}=\text{N})_{\text{Py}}$ ,<sup>[20]</sup> vibrations, respectively. The spectrum displayed four bands in the range  $1550$ - $1450 \text{ cm}^{-1}$  due to amide II, amide III, thioamide I, and thioamide II<sup>[15]</sup> (Figure 1). Furthermore, the band at  $844 \text{ cm}^{-1}$  was assigned to  $\nu(\text{C}=\text{S})$ ,<sup>[21]</sup> while those at  $777$  and  $757 \text{ cm}^{-1}$  were attributed to  $\rho(\text{NH})$ <sup>[21]</sup> vibration.

Thus, the above-mentioned spectral data clarify that  $\text{H}_3\text{L}$  exists in the keto-form where, NH, carbonyl, and thio-carbonyl vibrations appear. On comparison with isonicotinic hydrazide spectrum, it is observed that the  $\nu(\text{C}=\text{O})_{\text{Py}}$  vibration band shifted to higher position which may be due to involvement of carbonyl oxygen in intermolecular hydrogen bond with  $\text{N}^2\text{H}$  group where a new band at  $\sim 1965 \text{ cm}^{-1}$  were observed and attributed to intermolecular hydrogen bond.<sup>[22]</sup>

On the other hand, the spectral data of  $\text{H}_3\text{L}$  metal complexes (Table 2; Figure 2), indicate that all complexes have three bands in the ranges  $3410$ - $3398$ ,  $3265$ - $3245$ , and  $3185$ - $3140 \text{ cm}^{-1}$  attributed to  $\nu(\text{OH})_{\text{solvent}}$ <sup>[23]</sup>

$\nu(\text{N}^4\text{H})$ , and  $\nu(\text{N}^2\text{H})$ ,<sup>[16]</sup> respectively. The region  $1750$ - $1400 \text{ cm}^{-1}$  displayed overlapped bands and so deconvolution analyses were applied to resolve these bands (Table 3; Figure 3). The data showed weak band in the range  $1702$ - $1688 \text{ cm}^{-1}$  and a strong one in the range  $1645$ - $1620 \text{ cm}^{-1}$  assigned to  $\nu(\text{C}=\text{O})_{\text{Ph}}$ <sup>[15]</sup> and  $\nu(\text{C}=\text{N})_{\text{Py}}$ ,<sup>[20]</sup> respectively. In addition, a new band observed at  $1640$ - $1665 \text{ cm}^{-1}$  range, attributed to  $\nu(\text{C}=\text{N}^*)$ <sup>[16]</sup> vibration and two bands in the  $1534$ - $1511$  and  $1390$ - $1365 \text{ cm}^{-1}$  regions, assigned to  $\nu_{\text{as}}(\text{OAc})$  and  $\nu_{\text{s}}(\text{OAc})$  vibrations, respectively. It was suggested that acetate group coordinates in bidentate fashions where the difference between the asymmetric and symmetric vibrations is  $\approx 150 \text{ cm}^{-1}$ .<sup>[23-25]</sup> Furthermore, the spectra displayed new bands at  $585$ - $525$  and  $465$ - $435 \text{ cm}^{-1}$  which may be due to the  $\nu(\text{M}-\text{O})$  and  $\nu(\text{M}-\text{N})$ <sup>[26]</sup> vibrations, respectively. In comparison with the ligand spectrum, it could be concluded that the  $\text{H}_3\text{L}$  coordinates to the metal ions as mononegative bidentate (Figure 4) where: The disappearance of  $\nu(\text{N}^1\text{H})$  and  $\nu(\text{C}=\text{O})_{\text{Py}}$  bands with appearance of new  $\nu(\text{C}=\text{N}^*)$  band indicates

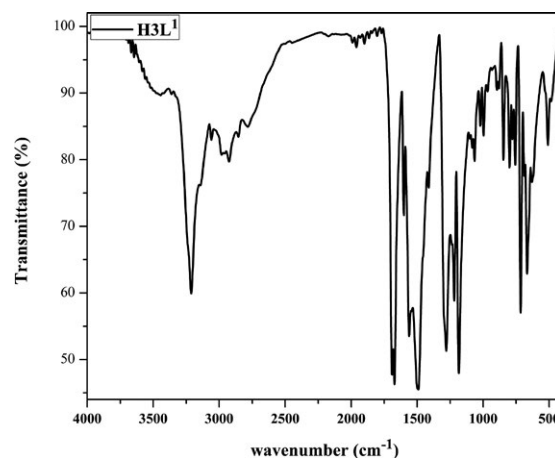


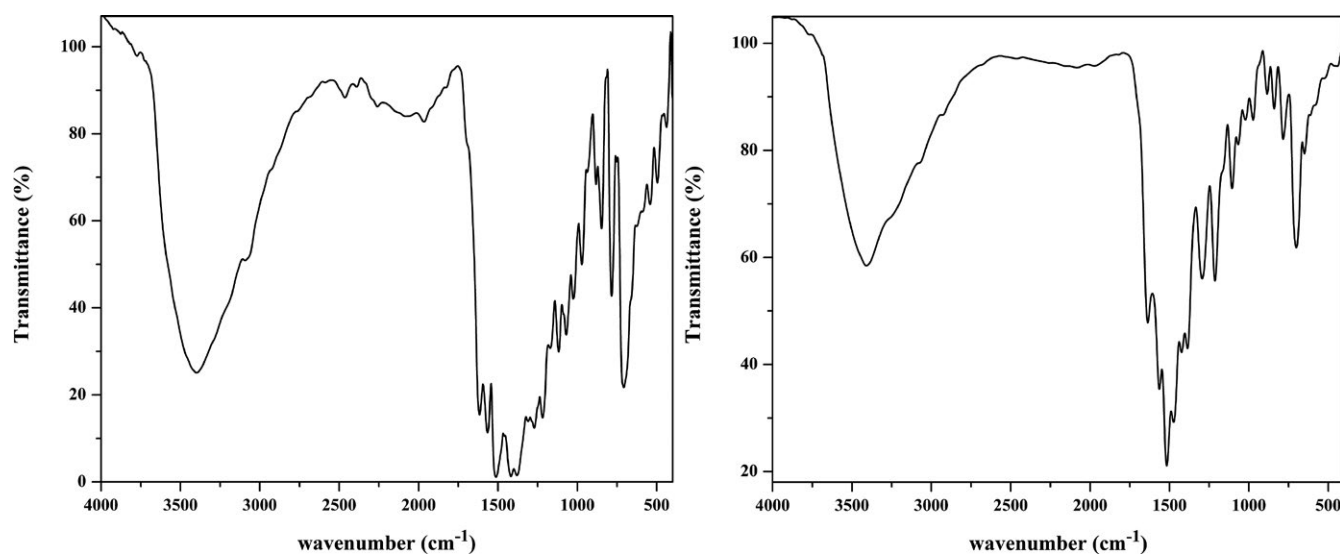
FIGURE 1 Infrared spectra of  $\text{H}_3\text{L}$

TABLE 1 Color, melting points and elemental analyses of the ligand and its metal complexes

Compound (Mol. Wt.)	Color	m.p. (°C)	Elemental analyses % found (Calcd.)		
			C	H	M
$\text{H}_3\text{L}$ (Calcd., 300.34; MS, 300)	Yellow	206	56.69 (55.99)	4.50 (4.03)	-
$[\text{Cu}(\text{H}_2\text{L})\text{Ac}] 3\text{H}_2\text{O}$ (Calcd., 475.99; MS, 477)	Black	>300	40.43 (40.37)	4.81 (4.24)	13.67 (13.35)
$[\text{Co}(\text{H}_2\text{L})\text{Ac}] 2\text{H}_2\text{O EtOH}$ (Calcd., 499.40; MS, 500)	Dark green	>300	43.90 (43.29)	5.55 (4.84)	11.90 (11.80)
$[\text{Ni}(\text{H}_2\text{L})\text{Ac}] 2\text{H}_2\text{O EtOH}$ (Calcd., 499.16; MS, 500)	Dark brown	>300	43.53 (43.31)	5.10 (4.85)	11.81 (11.76)
$[\text{Zn}(\text{H}_2\text{L})\text{Ac}] 2\text{H}_2\text{O EtOH}$ (Calcd., 505.47; MS, 506)	Green	>300	41.60 (41.78)	4.10 (3.91)	12.90 (12.28)

**TABLE 2** Infrared spectral data of  $H_3L$  and its isolated metal complexes

Vibration	$H_3L$	$Cu(II)-H_2L$	$Co(II)-H_2L$	$Ni(II)-H_2L$	$Zn(II)-H_2L$
$\nu(OH)_{\text{solvent}}$	-	3398	3407	3407	3411
$\nu(N^4H)$	3243	3245	3251	3245	3261
$\nu(N^2H)$	3211	3176	3170	3185	3145
$\nu(N^1H)$	3147	-	-	-	-
$\nu(C=O)_{Py}$	1672	-	-	-	-
$\nu(C=N)^a$	-	1665 <sup>a</sup>	1643 <sup>a</sup>	1642 <sup>a</sup>	1643 <sup>a</sup>
Amide II	1560	1557 <sup>a</sup>	1567 <sup>a</sup>	1558 <sup>a</sup>	1565 <sup>a</sup>
Amide III	1218	1218	1213	1216	1213
Thioamide I	1502	1517 <sup>a</sup>	1515 <sup>a</sup>	1519 <sup>a</sup>	1519 <sup>a</sup>
Thioamide II	1452	1421	1423	1421	1439
Thioamide III	1278	1272	1292	1288	1292
$\nu(C=S)$	844	848	840	844	842
$\rho(NH)$	777, 757	784, 709	782, 700	790, 717	798, 707
$\nu_{as}(OAc)$	-	1527 <sup>a</sup>	1528 <sup>a</sup>	1511 <sup>a</sup>	1534 <sup>a</sup>
$\nu_s(OAc)$	-	1374	1365	1374	1390
$\nu(M-O)$	-	588, 539	576, 524	576, 526	574, 514
$\nu(M-N)$	-	437	443	466	440

<sup>a</sup>Values estimated by deconvolution analyses.**FIGURE 2** Infrared spectra of  $[Cu(H_2L)Ac(H_2O)]_2H_2O$  and  $[Co(H_2L)Ac]_2H_2O \cdot EtOH$ 

the existence of the ligand in the enol form. The absence of the band due to  $\nu(OH)$  clarifies the deprotonation of the newly formed hydroxyl group on reaction with metal ion. The positions of the bands due to carbonyl group and the azomethine of the pyridyl ring did not change and so they are not involved in coordination. The appearance of  $\nu(C=S)$  vibration band approximately at the same position as in the ligand spectrum, indicates the inertness of thione sulfur toward coordination to the metal ions.

## 2.2 | $^1H$ and $^{13}C$ NMR spectra

$^1H$ -NMR of  $H_3L$ , in  $DMSO-d_6$ , exhibits several singlet signals corresponding to the protons of  $N^4H$ ,  $N^2H$ , and  $N^1H$  at 11.78, 10.73, and 8.80 ppm, respectively.<sup>[16]</sup> The appearance of these signals confirms the existence of the  $H_3L$  in the keto form. Multiplet signals observed in the region 7.98–7.21–7.31 ppm were assigned to the protons of the phenyl group (Table 4).<sup>[20]</sup> The pyridyl ring showed two doublet signals at 8.82 and 7.83 ppm, due to protons at (2 and 6) and (3 and 5) positions,<sup>[21]</sup> respectively.

**TABLE 3** Deconvolution analyses data of complexes infrared spectra in 1710-1400  $\text{cm}^{-1}$  range

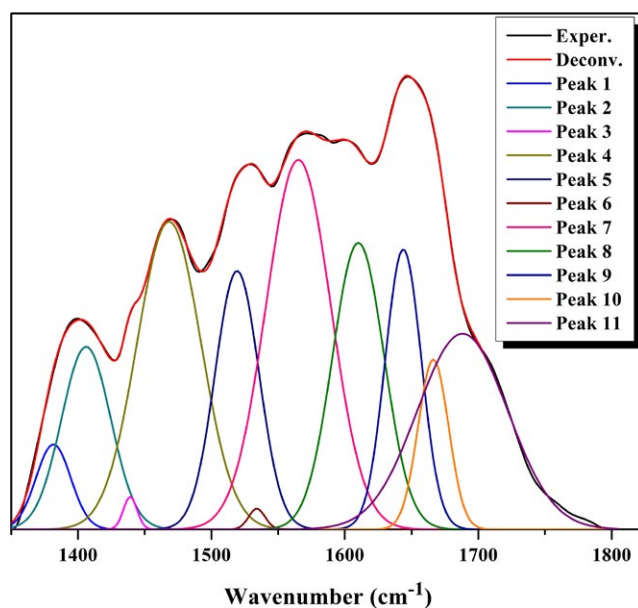
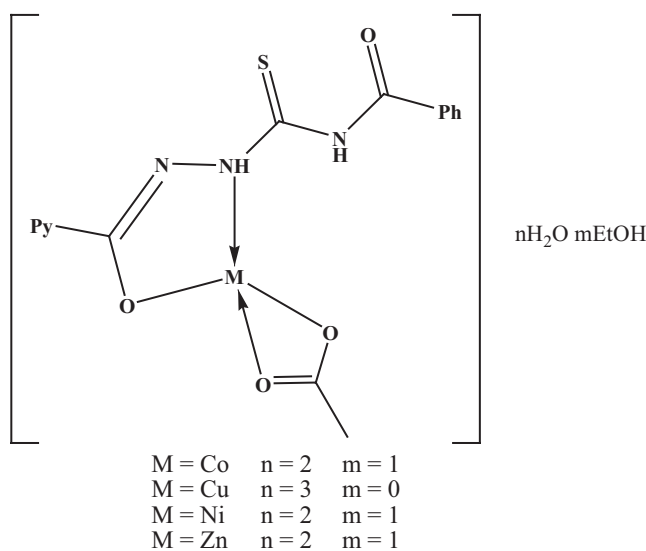
Peak	Co(II) complex ( $R^2 = 0.9999$ )			Ni(II) complex ( $R^2 = 0.9978$ )			Cu(II) complex ( $R^2 = 0.9990$ )		
	Center	FWHM	% Area	Center	FWHM	% Area	Center	FWHM	% Area
1	1460	16.48	2.11	1451	10.23	1.99	1507	41.05	14.36
2	1475	25.77	8.07	1483	25.82	10.07	1527	20.88	5.347
3	1515	37.51	22.12	1519	24.81	19.92	1557	17.29	3.23
4	1528	22.50	4.16	1558	12.09	3.05	1572	32.65	17.01
5	1567	34.69	18.63	1571	19.10	3.11	1620	50.02	49.22
6	1604	35.54	7.79	1606	20.81	5.63	1665	27.42	4.36
7	1643	44.47	35.18	1642	38.86	50.85	1699	30.43	6.44
8	1703	28.25	1.92	1701	32.37	5.34			

**TABLE 4** The NMR ( $^{13}\text{C}$  and  $^1\text{H}$ ) spectral data of ligands and Zn(II)-HL<sup>2</sup> complex

C-atoms	$^1\text{H-NMR}$			
	H <sub>3</sub> L	Protons	H <sub>3</sub> L	Zn(II)
2,6-pyridyl	150.32	N <sup>4</sup> H	11.78	11.44
3-pyridyl	121.52	N <sup>2</sup> H	11.43	-
5-pyridyl	121.52	N <sup>1</sup> H	8.80	-
4-pyridyl	139.34	2,6-pyridyl	8.82	7.73
2,6-phenyl	128.46	3,5-pyridyl	7.83	7.60
3,5-phenyl	128.72	2,6-phenyl	7.98	7.40
4-phenyl	131.84	3,5-phenyl	7.60	7.30
1-phenyl	133.18	4-phenyl	7.75	7.30
(C=O) <sub>Py</sub>	163.13			
(C=O) <sub>Ph</sub>	167.71			
(C=S)	181.03			
CH <sub>2</sub>	-			

$^1\text{H-NMR}$  of  $[\text{Zn}_2(\text{HL})\text{Ac}]2\text{H}_2\text{OEtOH}$  shows singlet signal at 11.34 ppm assigned to the proton of N<sup>4</sup>H group. In comparison with the ligand spectrum, it is clear that N<sup>2</sup>H signal has disappeared. The absence of N<sup>2</sup>H signal from the spectrum of Zn(II) complex confirms the coordination of the ligand in the enol form with liberation of hydrogen ion.<sup>[21]</sup> The singlet at 8.64 ppm was attributed N<sup>1</sup>H proton. The multiplet signals in the ring 7.45-8.52 ppm were attributed to the phenyl and pyridyl protons.

$^{13}\text{C-NMR}$  spectrum of H<sub>3</sub>L, in DMSO-d<sub>6</sub>, shows number of signals represent the number of chemically non-equivalent carbon atoms of H<sub>3</sub>L. The signal due to the carbonyl carbon adjacent to the pyridyl ring appears at 163.13 ppm, while the thiocarbonyl carbon was observed at  $\approx 182$  ppm.<sup>[21]</sup> The pyridyl ring carbons at 3-, 4-, and 5-positions were observed at  $\approx 121$ , 139, and 120 ppm, respectively, while those at 2- and 6-positions were at  $\approx 150$  ppm. The phenyl group carbon's displayed signals in the range 127.06-139.27 ppm (Table 4; Figure 5).<sup>[21]</sup>

**FIGURE 3** Deconvulsion analysis of  $[\text{Zn}(\text{H}_2\text{L})\text{Ac}] 2\text{H}_2\text{O EtOH}$ **FIGURE 4** Suggested structure of the metal complexes

### 2.3 | Electronic spectra and magnetic moments

The electronic spectrum of the ligand, in DMSO, showed two bands in the region 292–298 nm were attributed to ( $\pi \rightarrow \pi^*$ ) transitions of pyridine or phenyl, and carbonyl groups, respectively. Two shoulders locate at  $\approx 341$  and 365 nm due to ( $\pi \rightarrow \pi^*$ ) of thiocarbonyl and ( $n \rightarrow \pi^*$ ) of pyridine ring,<sup>[21]</sup> respectively. In addition, two bands were observed at 380 and  $\approx 390$  nm assigned to ( $n \rightarrow \pi^*$ ) transitions of carbonyl and thiocarbonyl groups,<sup>[21]</sup> respectively.

The spectrum of  $[\text{Co}(\text{H}_2\text{L})\text{Ac}] 2\text{H}_2\text{OEtOH}$  in DMSO showed only one band at 606 nm, attributed to  ${}^4\text{A}_2 \rightarrow {}^4\text{T}_1(\text{P})$  transition which suggests the tetrahedral geometry around the Co(II).<sup>[27]</sup> Another band at  $\approx 417$  nm was observed and assigned to the ligand to metal charge transfer transition (LMCT). Moreover, the spectral data of this complex in Nujol mull (Table 5) showed the d-d transition band at 615 nm confirming the tetrahedral structure of this solid complex and indicating that the use of DMF as solvent did not alter the geometrical structure. The magnetic moment of this complex was found to be 4.50 B.M., supporting the suggested tetrahedral stereochemistry.<sup>[27]</sup>

Moreover,  $[\text{Cu}(\text{H}_2\text{L})\text{Ac}] 3\text{H}_2\text{O}$  spectrum (Figure 6) recorded in DMSO and Nujol mull exhibited a broadband at

650 nm attributed to  ${}^2\text{B}_{1g} \rightarrow {}^2\text{E}_{1g}$  transition of a square planar geometry.<sup>[28–30]</sup> A band was observed also at 420 nm due to LMCT (Figure 6). The magnetic moment value of was 1.80 B.M. which lies in the normal range of Cu(II) complexes regardless of their stereochemistry (1.75–2.20 B.M.).

Furthermore, the spectrum of  $[\text{Ni}(\text{H}_2\text{L})\text{Ac}] 2\text{H}_2\text{O EtOH}$ , in DMSO, displayed two strong band at 422 and 500 nm attributed to the ligand to metal charge transfer transitions (LMCT). In addition, a broadband centered at 570 nm and a shoulder band at 700 nm assigned to  ${}^3\text{T}_1 \rightarrow {}^1\text{T}_1$  and  ${}^3\text{T}_1 \rightarrow {}^3\text{T}_1(\text{P})$  transitions, respectively. The position of these bands suggests tetrahedral geometry around Ni(II) ion.<sup>[27]</sup>

Moreover, the Nujol mull spectrum displayed the LMCT transitions at 450 and 540 nm, while two other transitions were observed at 550 and 707  $\text{cm}^{-1}$  due to  ${}^3\text{T}_1 \rightarrow {}^1\text{T}_1$  and  ${}^3\text{T}_1 \rightarrow {}^3\text{T}_1(\text{P})$  transitions, respectively. These transitions confirm the suggested tetrahedral structure of the Ni(II) complex in solid state. Furthermore, the magnetic moment value of the Ni(II) complex confirmed the tetrahedral geometry, where it were found to be 3.4 B.M. which lies in the range of tetrahedral structure (3.4–4.2 B.M.).<sup>[27]</sup>

Finally, the electronic spectral data of  $[\text{Zn}(\text{H}_2\text{L})\text{Ac}] 2\text{H}_2\text{O EtOH}$  in DMSO displayed intra-ligand transition as shown in Table 5. Three bands were observed at 306, 357, and 386 nm

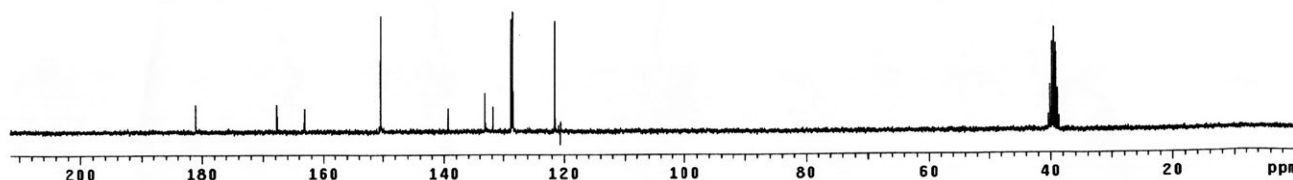


FIGURE 5 The  ${}^{13}\text{C}$ -NMR spectra of  $\text{H}_3\text{L}$

TABLE 5 Electronic spectral and magnetic moment data of ligands and its complexes

Compound	Band position (nm)	Assignment	$\mu_{\text{eff}}$ (B.M.)
$\text{H}_3\text{L}$	298, 306, 318, 352, 380, 388	$(\pi \rightarrow \pi^*)_{\text{Py}}$ , $(\pi \rightarrow \pi^*)_{\text{C}=\text{S}}$ , $(\pi \rightarrow \pi^*)_{\text{C}=\text{O}}$ , $(n \rightarrow \pi^*)_{\text{Py}}$ , $(n \rightarrow \pi^*)_{\text{C}=\text{S}}$ , $(n \rightarrow \pi^*)_{\text{C}=\text{O}}$	-
Cu complex	300 (296), 316, 350 (356), 362, 390 (404), 438 (460), 670 (632)	$(\pi \rightarrow \pi^*)_{\text{Ph}}$ , $(\pi \rightarrow \pi^*)_{\text{C}=\text{O}}$ , $(n \rightarrow \pi^*)_{\text{Py}}$ , $(n \rightarrow \pi^*)_{\text{C}=\text{S}}$ , $(n \rightarrow \pi^*)_{\text{C}=\text{O}}$ , LMCT, ${}^2\text{B}_{1g} \rightarrow {}^2\text{E}_{1g}$	1.8
Co complex	296, 310 (304), 356 (360), 400 (386), 500 (498), 606 (615)	$(\pi \rightarrow \pi^*)_{\text{Py}}$ , $(\pi \rightarrow \pi^*)_{\text{C}=\text{S}}$ , $(n \rightarrow \pi^*)_{\text{Py}}$ , $(n \rightarrow \pi^*)_{\text{C}=\text{O}}$ , LMCT, ${}^4\text{A}_2 \rightarrow {}^4\text{T}_1(\text{P})$	4.50
Ni complex	302, 308 (316), 348, 356 (374), 396, 422 (450), 500 (504), 570 (550), 700 (708)	$(\pi \rightarrow \pi^*)_{\text{Ph}}$ , $(\pi \rightarrow \pi^*)_{\text{C}=\text{S}}$ , $(n \rightarrow \pi^*)_{\text{Py}}$ , $(n \rightarrow \pi^*)_{\text{C}=\text{S}}$ , $(n \rightarrow \pi^*)_{\text{C}=\text{O}}$ , LMCT, ${}^3\text{T}_1 \rightarrow {}^1\text{T}_1$ , ${}^3\text{T}_1 \rightarrow {}^3\text{T}_1(\text{P})$	3.14
Zn complex	282, 302, 318, 340, 364, 390, 470	$(\pi \rightarrow \pi^*)_{\text{Py}}$ , $(\pi \rightarrow \pi^*)_{\text{Ph}}$ , $(\pi \rightarrow \pi^*)_{\text{C}=\text{O}}$ , $(n \rightarrow \pi^*)_{\text{Py}}$ , $(n \rightarrow \pi^*)_{\text{C}=\text{S}}$ , $(n \rightarrow \pi^*)_{\text{C}=\text{O}}$ , LMCT	-

Value between brackets was from Nujol mull spectrum.

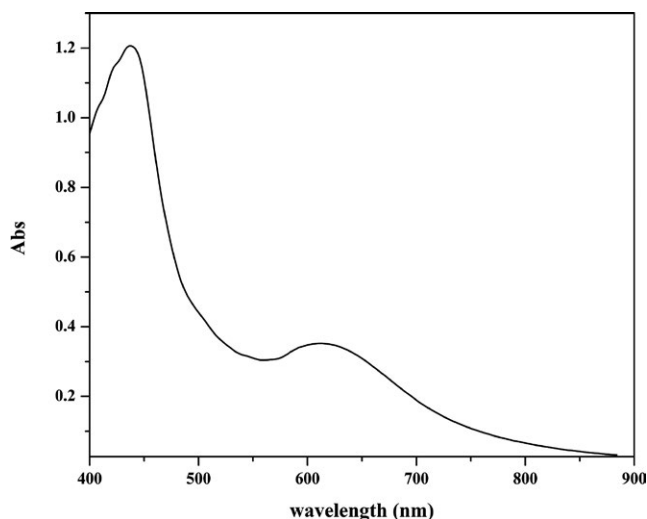


FIGURE 6 Electronic spectrum of  $[\text{Cu}(\text{H}_2\text{L})\text{Ac}]3\text{H}_2\text{O}$

attributed to  $(\pi \rightarrow \pi^*)_{\text{Ph}}$ ,  $(n \rightarrow \pi^*)_{\text{Py}}$ , and  $(n \rightarrow \pi^*)_{\text{C}=\text{N}^*}$ , respectively. In addition to LMCT bands at 434 and 504 nm. The obscure of the bands due to  $\pi \rightarrow \pi^*$  and  $n \rightarrow \pi^*$  transitions of carbonyl was taken as an additional evidence for enolization of this group.

## 2.4 | ESR spectra of Cu(II) complex

ESR is important technique for determining the stereochemistry of Cu(II) complexes. The ground state is  $d_{z^2}$  in octahedral or a trigonal bipyramidal Cu(II) complexes with  ${}^2\text{A}_{1g}$  ground state. The ESR can distinguish the ground states according to the values of the  $g$ -tensor. Thus, when  ${}^2\text{B}_{1g}$  is the ground state the  $g_{\parallel} > g_{\perp} > 2.0023$ , while in case of  ${}^2\text{A}_{1g}$  ground state the  $g_{\perp} > g_{\parallel} > 2.0023$ .<sup>[31]</sup>

From ESR spectrum of Cu(II) complex (Figure 7), it was found that,  $g_{\parallel} = 2.20$  and  $g_{\perp} = 2.08$ . From these observed values it could be deduced that;  $g_{\parallel}$  is less than 2.3 suggesting a significant covalent character of metal-ligand bonds.<sup>[32]</sup> The obtained  $g$ -values are  $g_{\parallel} > g_{\perp} > 2.0023$  which means that the Cu(II) has a  $d_{x^2-y^2}$  ground state characteristic for square planar geometry.<sup>[33]</sup> The exchange interaction between Cu(II) centers may be expressed by the axial symmetry parameter,  $G$ , where  $G = (g_{\parallel} - 2)/(g_{\perp} - 2)$ . The  $G$  value was found to be 2.41, suggesting considerable copper-copper exchange interactions in the solid state.<sup>[28]</sup>

The orbital reduction factor,  $\mathbf{K}$ , was used as a measure of covalency, where for ionic environment  $K = 1$ , and for covalent  $K < 1$ . The orbital reduction factor is calculated using the following expressions<sup>[29]</sup> where  $K_{\parallel}$ ,  $\mathbf{K}_{\perp}$ , parallel, perpendicular components of orbital reduction factor and  $\lambda_o$  is the spin-orbit coupling constant.

$$K_{\parallel}^2 = \frac{g_{\parallel} - 2.0023}{8 \times \lambda_o} \times d-d \text{ transition}$$

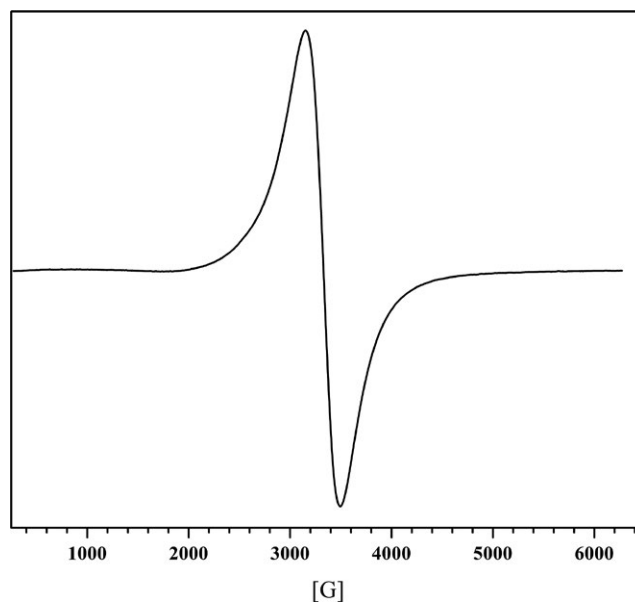


FIGURE 7 ESR spectra of  $[\text{Cu}(\text{H}_2\text{L})\text{Ac}]2\text{H}_2\text{O}$

$$K_{\perp}^2 = \frac{g_{\perp} - 2.0023}{2 \times \lambda_o} \times d-d \text{ transition}$$

$$K^2 = \frac{K_{\parallel}^2 + 2K_{\perp}^2}{3}$$

The pure  $\sigma$ -bonding  $K_{\parallel} \approx K_{\perp} \approx 0.77$  and for in-plane  $\pi$ -bonding  $K_{\parallel} < K_{\perp}$ , while for out-of-plane  $\pi$ -bonding  $K_{\parallel} > K_{\perp}$ . The obtained data are shown Table 6. The results indicated that Cu(II) complex has  $\mathbf{K} < 1$  and  $K_{\parallel} < K_{\perp}$ , so they have covalent environment and in-plane  $\pi$ -bonding.

Finally, the magnetic moment for the Cu(II) complexes,  $\mu_{\text{eff}}$ , can be calculated using the ESR data,  $g$ -values, by the following expression.<sup>[30]</sup> The data indicated that it is very close to obtained value from magnetic susceptibility measurements (1.80 B.M.) and found to be 1.84 B.M., respectively.

$$\mu_{\text{eff}} = \frac{1}{2} \sqrt{g_{\parallel}^2 + 2g_{\perp}^2}$$

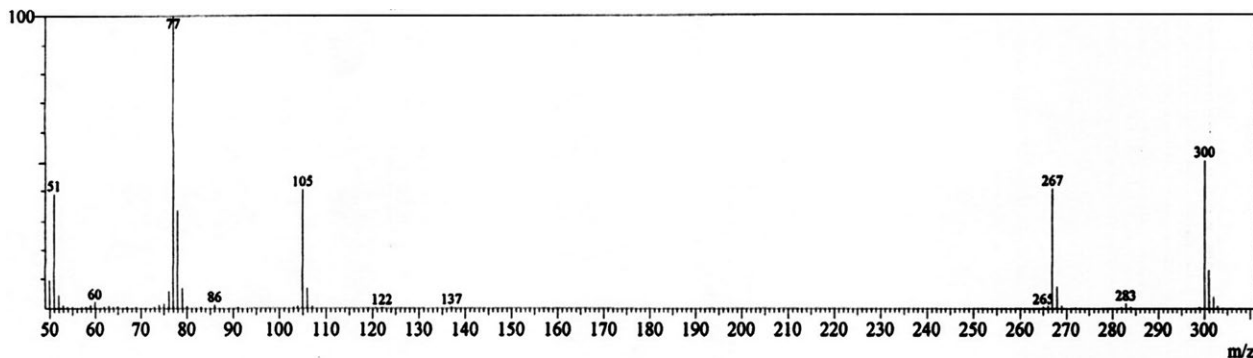
## 2.5 | Mass spectra

The mass spectrum of the  $\text{H}_3\text{L}$  ligand shows the molecular ion peak at  $m/z = 300$  (60.0%), which matches with the suggested formula (Figure 8). The ligand loses  $\text{HO}^-$  ion giving a peak at  $m/z = 283$  (2.5%) which undergoes two different fragmentation pathways to base peak at  $m/z = 77$  (100.0%) corresponding to either pyridyl or phenyl ring (Scheme 1).

The spectrum showed peak at  $m/z = 268$  (3.0%) resulted from loss of oxygen from the peak at  $m/z = 283$ . The latter peak may lose sulfur to give another peak at  $m/z = 251$  (1.3%) or loses  $\text{C}_7\text{H}_7\text{N}$  fragments to give a third peak at  $m/z = 178$  (0.3%).

**TABLE 6** ESR and orbital reduction parameters of Cu(II) complexes

Complex	$g_{\parallel}$	$g_{\perp}$	G	$\mu_{\text{eff}}$	$K_{\parallel}^2$	$K_{\perp}^2$	$K^2$	$K_{\parallel}$	$K_{\perp}$	K
Cu-H <sub>3</sub> L	2.20	2.09	2.41	1.84	0.49	0.82	0.71	0.70	0.90	0.84

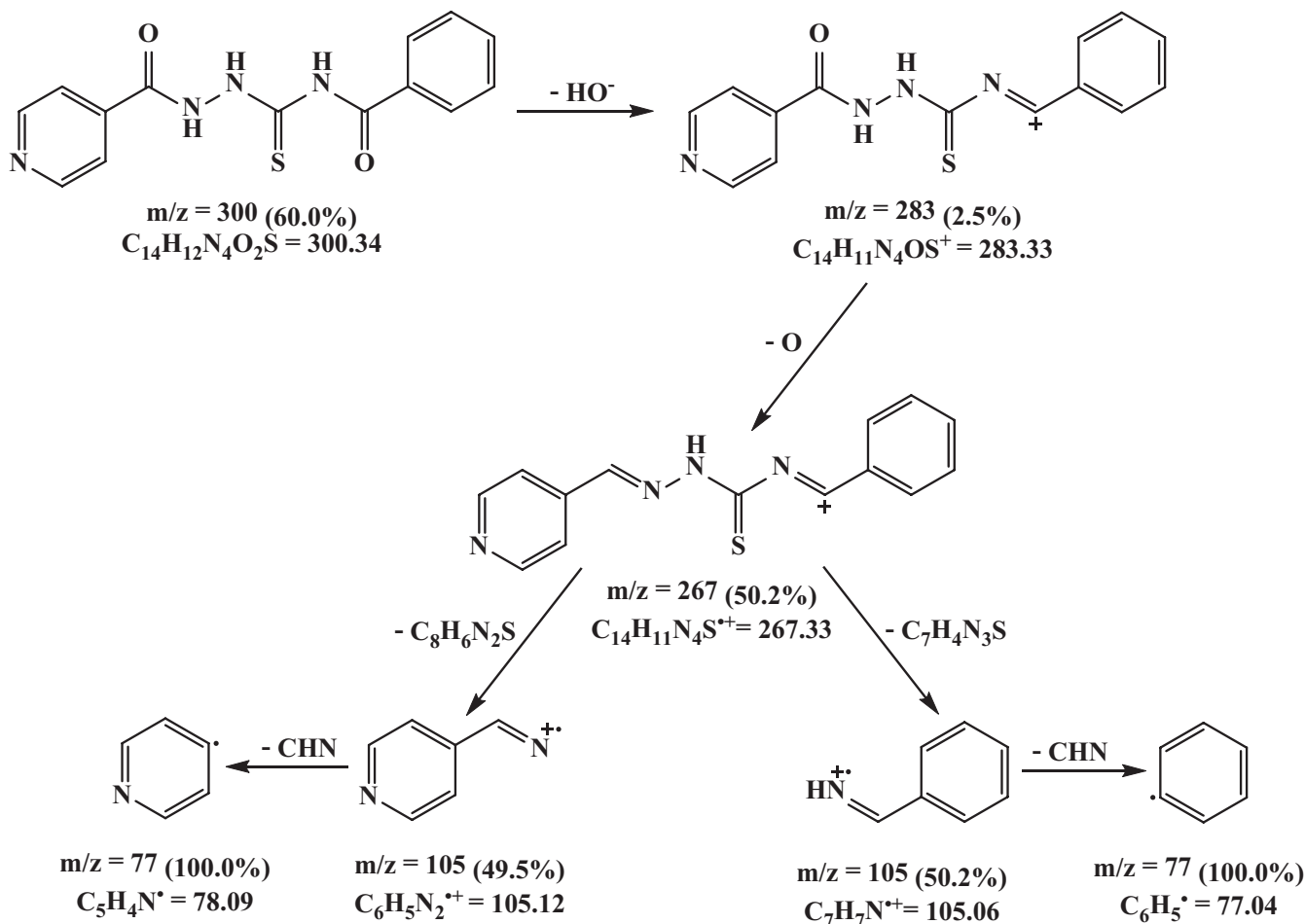
**FIGURE 8** Mass spectrum of H<sub>3</sub>L

## 2.6 | Thermal analyses

Thermal gravimetric analysis (TGA) for the obtained solid complexes were carried out to clarify their thermal stability and to help in characterization. In Table 7, the decomposition

steps of each complex were listed. The TG data indicated that: In general the first step, water and/or ethanol molecules out the coordination sphere were lost in temperature range 20–170°C.

In the second stage ranged from 101 to 400°C, the acetate molecules were lost.

**SCHEME 1** Fragmentation pattern of H<sub>3</sub>L

The kinetics and thermodynamic parameters, activation energy ( $E_a$ ), enthalpy ( $\Delta H^*$ ), entropy ( $\Delta S^*$ ), and free energy ( $\Delta G^*$ ) change of decomposition are evaluated graphically by employing Coats-Redfern<sup>[34]</sup> and Horowitz-Metzger<sup>[35]</sup> methods. The data obtained were collected in Table 8. The results indicated the following remarks:

For all complexes, these methods were applicable on the first decomposition stage corresponding to loss of solvent molecules outside the coordination sphere, which clarifies that it is simple and has moderate rate. Other decomposition stages do not fit the requirements for applying the calculation methods, due to the overlapped stages, except in case of Ni(II) and Zn(II) complexes.

The  $E_a$  values for the first step obtained from Coats-Redfern method are considerably close to those from Horowitz-Metzger method. For all complexes, the obtained  $E_a$  values of the first step were close and in the range 25–57 kJ.

The negative values of  $\Delta S^*$  indicate that the activated fragments have more ordered structure than the undecomposed complexes and/or the decomposition reactions are slow. The positive sign of  $\Delta H^*$  reveals that the decomposition stages are endothermic processes.<sup>[36]</sup>

The positive sign of  $\Delta G^*$  indicates that the free energy of the resulting formula is higher than that of the initial

**TABLE 7** Thermal gravimetry analysis data of metal complexes

Complex	Temp. range	Wt. loss %	Fragment loss	Fragment %
[Cu(H <sub>2</sub> L)Ac]3H <sub>2</sub> O (475.99)	20-120	11.47	3H <sub>2</sub> O	11.34
	101-283	13.03	C <sub>2</sub> H <sub>3</sub> O <sub>2</sub>	12.39
	283-415	35.30	C <sub>11</sub> H <sub>11</sub> N	35.76
	415-1000	9.58	NS	9.66
	Residue	30.31	CuC <sub>3</sub> HNO <sub>2</sub>	30.81
[Co(H <sub>2</sub> L)Ac]2H <sub>2</sub> O EtOH (499.40)	20-150	16.38	EtOH and 2H <sub>2</sub> O	16.41
	151-395	18.01	C <sub>2</sub> H <sub>4</sub> O <sub>2</sub> S	18.66
	395-575	30.47	C <sub>11</sub> H <sub>11</sub> N	31.08
	530-1000	9.62	CO <sub>2</sub>	8.81
	Residue	24.52	CoC <sub>2</sub> HN <sub>3</sub>	25.23
[Ni(H <sub>2</sub> L)Ac]2H <sub>2</sub> O EtOH (499.16)	20-160	17.03	EtOH and 2H <sub>2</sub> O	16.42
	260-595	32.87	C <sub>8</sub> H <sub>5</sub> N <sub>2</sub> O <sub>2</sub>	32.69
	595-1000	14.06	C <sub>6</sub> H <sub>5</sub>	15.45
	Residue	36.04	NiC <sub>2</sub> H <sub>2</sub> N <sub>2</sub> O <sub>2</sub> S	35.41
[Zn(H <sub>2</sub> L)Ac]2H <sub>2</sub> O EtOH (505.47)	20-170	17.74	EtOH and 2H <sub>2</sub> O	16.22
	277-372	25.76	C <sub>2</sub> H <sub>3</sub> O <sub>2</sub> and C <sub>6</sub> H <sub>5</sub>	26.90
	372-550	19.63	C <sub>7</sub> H <sub>6</sub> N	20.57
	550-1000	7.92	CS	8.70
	Residue	29.45	ZnN <sub>3</sub> O <sub>2</sub>	30.35

**TABLE 8** Thermodynamic parameters data of metal complexes

Complex	Temp. range	Thermodynamic parameters					
		$E_a$ (kJ)	$\Delta S^*$ (J mol <sup>-1</sup> K <sup>-1</sup> )	$\Delta H^*$ (kJ)	$\Delta G^*$ (kJ)	A	R
[Cu(H <sub>2</sub> L)Ac]3H <sub>2</sub> O	20-215	48.78 (57.79)	-201.87	46.01	113.42	198.44	0.973 (0.953)
[Co(H <sub>2</sub> L)Ac]2H <sub>2</sub> O EtOH	20-135	41.51 (46.44)	-232.40	37.46	150.64	7.35	0.970 (0.957)
[Ni(H <sub>2</sub> L)Ac]2H <sub>2</sub> O EtOH	20-120	44.06 (49.92)	-219.13	41.21	116.54	25.62	0.980 (0.964)
	120-369	33.05 (45.77)	-301.41	28.74	185.16	0.002	0.985 (0.966)
[Zn(H <sub>2</sub> L)Ac]2H <sub>2</sub> O	277-372	72.24 (85.79)	-234.42	67.28	207.34	7.08	0.971 (0.974)
	372-550	72.08 (83.08)	-259.52	65.94	257.63	0.427	0.966 (0.971)
	550-1000	73.94 (97.19)	-303.46	65.41	376.93	0.003	0.973 (0.981)

Values in brackets obtained by Horowitz-Metzger.

compound, and hence all the decomposition steps are non-spontaneous processes. Moreover, the values of  $\Delta G^*$  increase significantly for the subsequent decomposition stages of a given compound. This observation is a result of increasing of TΔS, which reflects the lower rate of removal of the subsequent species compared with the precedent one.<sup>[37]</sup>

## 2.7 | Optical band gap

Molecular materials can be used in molecular electronics due to their conducting and semi-conducting nature.<sup>[38-41]</sup> To have an idea on the conductivity of the current metal complexes, the optical band gaps ( $E_g$ ) have been measured from the electronic spectra. Tauc's relation (1) has been applied:  $\alpha h\nu = A (h\nu - E_g)^m$  (1), where  $m$  is equal to 2 for direct electronic transition,  $A$  is a constant.<sup>[42,43]</sup> Representative examples of the optical band gap ( $E_g$ ) curves of the ligand and its metal complexes are represented in Figure 9. The results indicated that  $E_g$  values of  $H_3L$  and its metal complexes are in the range 3.82-3.85 eV. These values are in good agreement with some semi-conducting materials.<sup>[44-48]</sup>

## 2.8 | Cytotoxic effect

The in vitro cytotoxicity activities of  $H_3L$  and its Zn(II) complex are studied as representative examples of the present compounds.

The cytotoxicity activity against human tumor cells and the relative viability are collected in Tables 9 and 10 (Figure 10). The results indicated that the minimum inhibitory concentration of  $H_3L$  found to be 11.32 and 7.80  $\mu\text{g/mL}$  against HCT-116 and HEPG-2 cell lines, respectively. On the other hand, the minimum inhibitory concentration of Zn(II) complexes was found to be 30.60 and 25.9  $\mu\text{g/mL}$  against HCT-116 and HEPG-2 cell lines.

The cytotoxicity tests showed that the  $H_3L$  has very strong cytotoxic effect against HePG-2 while, it shows strong cytotoxicity against HCT-116. The Zn(II) complex showed moderate cytotoxicity against the two cell lines.

Compared with other isonicotinic derivative (2-isonicotinoyl-*N*-phenylhydrazine-1-carboxamide),<sup>[16]</sup>  $H_3L$  has higher cytotoxicity activity than 2-isonicotinoyl-*N*-phenylhydrazine-1-carboxamide. The structure of  $H_3L$  has thione group (C=S) in place of carbonyl group in the compound under comparison. It could be concluded that the higher activity of  $H_3L$  resulted from the presence of the thione group.

## 3 | CONCLUSION

The free ligand, 4-benzyl-thiosemicarbazide ( $H_3L$ ) exists in keto-thio keto form.  $H_3L$  chelates to Cu(II), Co(II),

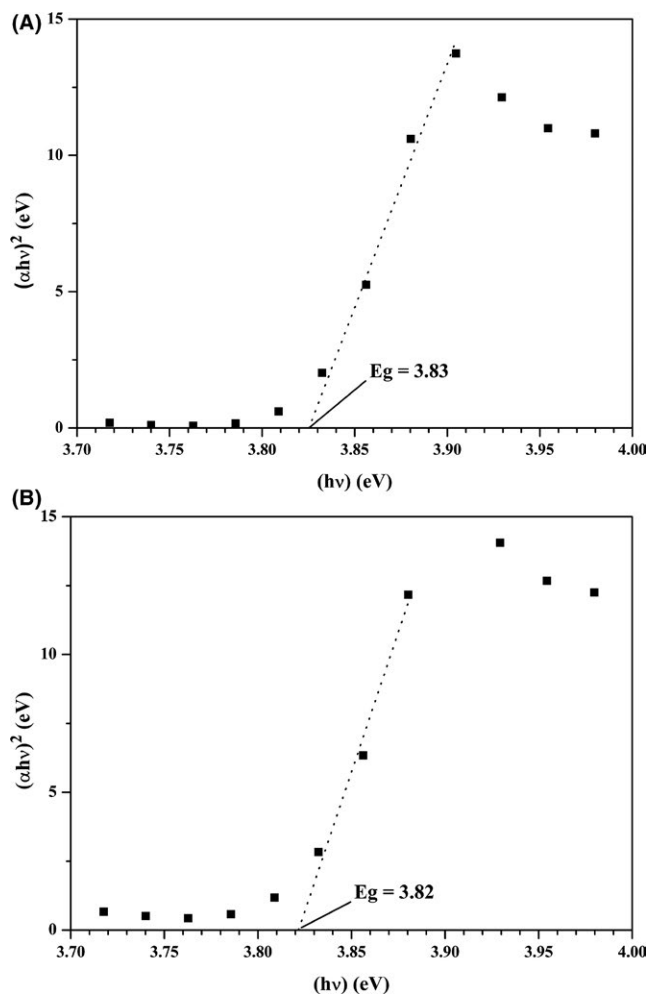


FIGURE 9 Energy gap plots of  $H_3L$  (A) and (B) Cu(II) complex

TABLE 9 Cytotoxic activity of some compounds against human tumor cells

Compounds	In vitro Cytotoxicity IC <sub>50</sub> ( $\mu\text{g/mL}$ ) <sup>a</sup>	
	HCT116	HePG2
DOX	5.23 $\pm$ 0.3	4.50 $\pm$ 0.2
$H_3L$	11.32 $\pm$ 1.1	8.90 $\pm$ 0.8
Zn complex	34.60 $\pm$ 2.0	26.20 $\pm$ 1.7

DOX, Doxorubicin.

<sup>a</sup>IC<sub>50</sub> ( $\mu\text{g/mL}$ ): 1-10 (very strong), 11-20 (strong), 21-50 (moderate), 51-100 (weak), and above 100 (non-cytotoxic).

Ni(II), and Zn(II) in the enol form.  $H_3L$  reacts with metal ions as mononegative bidentate via the nitrogen atom of NH group, deprotonated oxygen of the enolized carbonyl. The electronic spectra and magnetic data of the isolated solid complexes indicated the formation of tetrahedral stereochemistry with all metal ions, except Cu(II) which forms square planar structure. The optical band gap measurements indicated that the ligand and its metal complexes

Conc. ( $\mu\text{g/mL}$ )	DOX		$\text{H}_3\text{L}$		$\text{Zn(II)}$	
	HCT116	HePG2	HCT116	HePG2	HCT116	HePG2
100	7.1	6.3	11.3	7.8	30.6	25.9
50	13.9	11.2	18.9	16.3	41.9	37.8
25	18.7	14.1	30.7	24.5	53.8	48.1
12.5	31.4	28.3	43.8	38.4	67.2	62.3
6.25	47.9	45.8	61.2	55.1	86.5	75.2
3.125	60.5	57.6	82.3	78.3	99.4	94.7
1.56	73.8	71.2	98.6	94.2	100	100

**TABLE 10** Relative viability of cells (%)

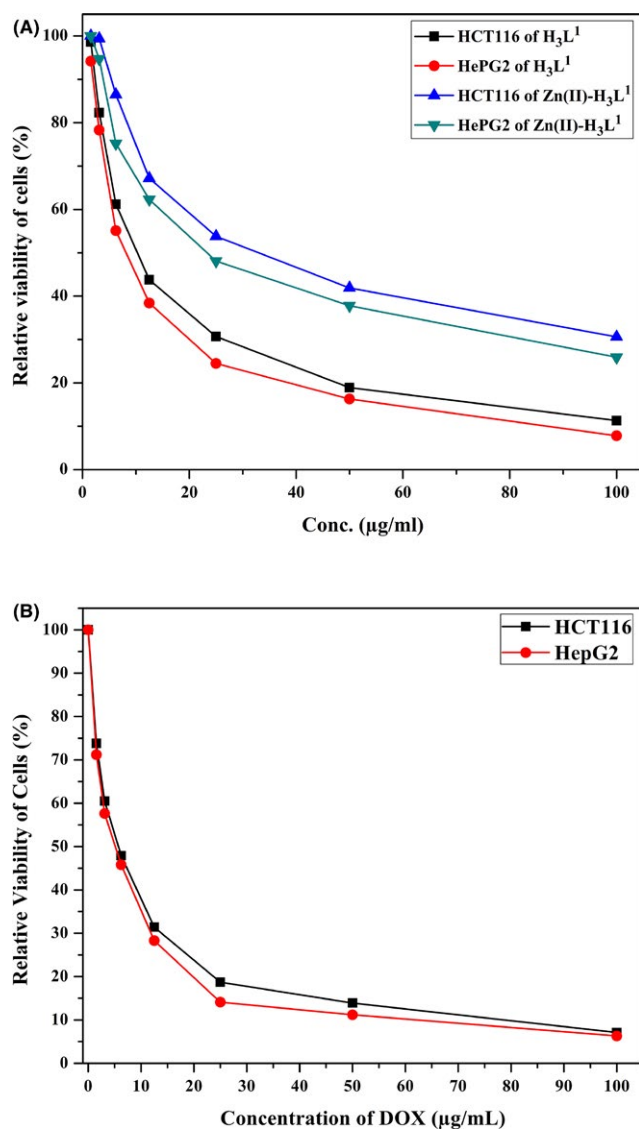


**FIGURE 10** In vitro cytotoxic activities of  $\text{H}_3\text{L}$  (A) and its  $\text{Zn(II)}$  complexes compared with the standard doxorubicin (B)

are semiconductors and could be used in solar cell applications. The ligand showed higher anti-cancer activity than its  $\text{Zn(II)}$  complex.

## 4 | EXPERIMENTAL

### 4.1 | Reagents

Isonicotinic hydrazide (99.0%) and benzoylisothiocyanate (98.0%) were purchased from Sigma-Aldrich. All the other used reagents are AR grade and used as it is.

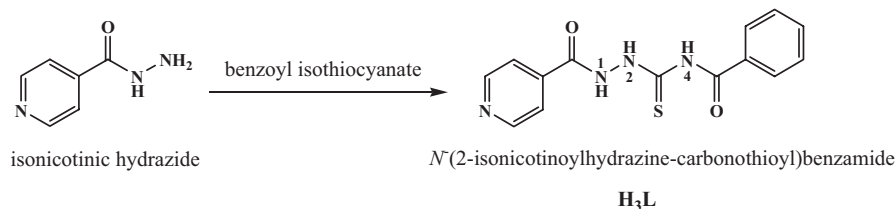
Cell lines, Colorectal (HCT-116), and Hepatocellular (HePG-2) carcinoma were obtained from ATCC via (VACSERA), Cairo, Egypt. The reagents RPMI-1640 medium, MTT, and 5-fluorouracil (Sigma Co., St. Louis, USA), Fetal Bovine serum (GIBCO, UK).

### 4.2 | Measurements

The elemental analyses (C, H, and N) were determined on CHN analyzer (Perkin-Elmer model 2400). The metal content was determined by direct titration against EDTA using suitable indicators for the analyzed metal ions.<sup>[49]</sup> The FT-IR spectra were recorded, as KBr disks, on a Thermo Nicolet IS10 spectrometer. TGA was carried out on a Shimadzu model 50 instrument with heating rate  $10^\circ\text{C}/\text{min}$  and  $20\text{ cm}^3/\text{min}$  nitrogen flow rate. The UV-Visible measurements were taken by Unicamy UV/Vis spectrometer UV2, with 1 cm silica cells. The NMR ( $^1\text{H}$  and  $^{13}\text{C}$ ) spectra were recorded on Bruker Ascend 400 MHz. Electron spin resonance (ESR) was recorded at room temperature on Bruker E 500 ESR spectrometer operating at 9.808 GHz, 100 kHz field. Modulation from 480 to 6480 Gauss in a 2 mm quartz capillary. Magnetic measurements were measured on a Sherwood Scientific magnetic balance. Molar conductivity was carried out on a conductivity bridge YSI model 32.

### 4.3 | Deconvolution analysis of infrared spectral data

Deconvolution analysis of the infrared spectra were calculated by the Peak Fit program to determine the hidden peaks at wavenumber different from local maximum in the data



SCHEME 2 Preparation of the ligand

stream.<sup>[50]</sup> The spectra were corrected for the dark current noises and background firstly. Spectral Gaussian peaks were used to obtain the best-fitted data. The intensity, full width at half maximum (FWHM) and position of each band were adjusted automatically by the program, on the basis of the minimization of the deviations between experimental and simulated spectrum.<sup>[51,52]</sup>

#### 4.4 | Synthesis of the ligand ( $H_3L$ )

Isonicotinic hydrazide (0.01 mol) was dissolved in 25 mL ethanol and to which benzoylisothiocyanate (0.01 mol) was added dropwise. The reaction mixture was refluxed for 1 hour. After cooling to room temperature, white crystals were precipitated. After filtration the precipitate was washed with ethanol and dried in air (m.p.: 232°C). The formation reaction of the ligand is shown in Scheme 2.

#### 4.5 | Synthesis of the metal complexes

The equivalent amount of the divalent copper, cobalt, nickel, and zinc acetates (0.01 mol) were dissolved in 25 mL absolute ethanol, then, added dropwise with stirring to the hot solution of  $H_3L$  (0.01 mol). Colored precipitates were formed on addition. The mixtures were filtered off while hot, washed successfully with ethanol, and dried in air.

#### 4.6 | Cytotoxicity assay

The cell lines HePG-2 and HCT-116 were used to measure the inhibitory effects of the ligand ( $H_3L$ ) and its Zn(II) complex on cell growth using the colorimetric assay MTT. This method is based on the conversion of the yellow color of tetrazolium bromide (MTT) to the purple color of formazan derivative by mitochondrial succinate dehydrogenase in viable cells. RPMI-1640 medium with 10% fetal bovine serum was used to culture the cell lines. The added antibiotics were 100  $\mu$ g/mL Streptomycin and 100 units/mL Penicillin in a 5%  $CO_2$  incubator at 37°C. The cell lines were seeded in a 96-well plate at a density of  $1.0 \times 10^4$  cells/well at 37°C for 48 h under 5%  $CO_2$ . After incubation, the cells were treated with different concentration of  $H_3L$  and its Zn complex and incubated for 24 hour. After drug treatment, 20  $\mu$ L of MTT solution at 5 mg/mL was added and incubated for 4 hour.

100  $\mu$ L dimethyl sulfoxide (DMSO) was added to each well to dissolve the purple color of the formed formazan. The readings were taken at 570 nm by a plate reader (EXL 800, USA). The relative cell viability in percentage was calculated as  $(A_{570}$  of treated samples/ $A_{570}$  of untreated sample)  $\times$  100. For comparison, Doxorubicin was used as a standard anticancer drug.<sup>[53,54]</sup>

#### ORCID

Nasser Mohammed Hosny  <http://orcid.org/0000-0003-1035-1480>

#### REFERENCES

- [1] M. Malhotra, M. Sanduja, A. Samad, A. Deep, *J. Serb. Chem. Soc.* **2012**, *77*, 9.
- [2] E. Pahontu, D. C. Ilies, S. Shova, C. Oprean, V. Paunescu, O. T. Olaru, F. S. Radulescu, A. Gulea, T. Rosu, D. Draganescu, *Molecules* **2017**, *22*, 650.
- [3] N. Fahmi, R. Singh, *J. Indian Chem. Soc.* **1996**, *73*, 257.
- [4] J. R. Dimmock, R. N. Puthucode, J. M. Smith, M. Hetherington, J. W. Quail, U. Pugazhenthii, T. Lechler, J. P. Stables, *J. Med. Chem.* **1996**, *39*, 3984.
- [5] J. Dimmock, K. Sidhu, S. Tumber, S. Basran, M. Chen, J. Quail, J. Yang, I. Rozas, D. Weaver, *Eur. J. Med. Chem.* **1995**, *30*, 287.
- [6] J. Dimmock, S. Pandeya, J. Quail, U. Pugazhenthii, T. Allen, G. Kao, J. Balzarini, E. DeClercq, *Eur. J. Med. Chem.* **1995**, *30*, 303.
- [7] T. S. Lobana, R. Sharma, G. Bawa, S. Khanna, *Coord. Chem. Rev.* **2009**, *253*, 977.
- [8] N. Nawar, E. El-Sawaah, N. M. Hosny, M. M. Mostafa, *Phosphorus Sulfur* **2012**, *187*, 976.
- [9] K. Uesugi, L. J. Sik, H. Nishioka, T. Kumagai, T. Nagahiro, *Microchem. J.* **1994**, *50*, 88.
- [10] N. Farrell, *Coord. Chem. Rev.* **2002**, *232*, 1.
- [11] D. L. Klayman, J. P. Scovill, J. F. Bartosevich, J. Bruce, *J. Med. Chem.* **1983**, *26*, 35.
- [12] R. M. Roat-Malone, *Bioinorganic Chemistry: A Short Course*, John Wiley & Sons, Hoboken, NJ **2007**.
- [13] N. K. Singh, S. B. Singh, *Transition Met. Chem.* **2001**, *26*, 487.
- [14] R. Rastogi, M. Yadav, K. Singh, *Synth. React. Inorg. Met. Org. Chem.* **2003**, *33*, 1585.
- [15] M. I. Orif, M. H. Abdel-Rhman, *Polyhedron* **2015**, *98*, 162.
- [16] N. M. Hosny, N. Y. Hassan, H. M. Mahmoud, M. H. Abdel-Rhman, *J. Mol. Struct.* **2018**, *1156*, 602.
- [17] M. Joseph, M. Kuriakose, M. P. Kurup, E. Suresh, A. Kishore, S. G. Bhat, *Polyhedron* **2006**, *25*, 61.

- [18] N. M. Hosny, Y. E. Sherif, *Spectrochim. Act.* **2015**, *136*, 510.
- [19] N. M. Hosny, A. M. Shallaby, *Transition Met. Chem.* **2007**, *32*, 1085.
- [20] R. Silverstein, F. Webster, *Spectrometric Identification of Organic Compounds*, John Wiley & Sons, Hoboken, NJ **2006**.
- [21] M. M. Mostafa, *Spectrochim. Act.* **2007**, *66*, 480.
- [22] M. H. Abdel-Rhman, M. M. Hassanian, A. A. El-Asmy, *J. Mol. Struct.* **2012**, *1019*, 110.
- [23] K. Nakamoto, *Infrared and Raman Spectra of Inorganic and Coordination Compounds*, Wiley Online Library, Hoboken, NJ **1978**.
- [24] A. A. El-Asmy, T. H. Rakha, M. H. Abdel-Rhman, M. M. Hassanien, A. S. Al-Mola, *Spectrochim. Act.* **2015**, *136*, 1718.
- [25] A. A. El-Asmy, M. M. Hassanian, M. H. Abdel-Rhman, *J. Sulfur Chem.* **2010**, *31*, 141.
- [26] G. Y. Nagesh, B. H. M. Mruthyunjayaswamy, *J. Mol. Struct.* **2015**, *1085*, 198.
- [27] A. B. P. Lever, *Inorganic Electronic Spectroscopy*, Elsevier, New York, NY **1968**.
- [28] G. Speier, J. Csihony, A. M. Whalen, C. G. Pierpont, *Inorg. Chem.* **1996**, *35*, 3519.
- [29] B. Hathaway, *Structure and Bonding*, Vol. 1, Springer Verlag, Berlin **1973**, 60.
- [30] V. T. Kasumov, F. Köksal, R. Köseoğlu, *J. Coord. Chem.* **2004**, *57*, 591.
- [31] B. J. Hathaway, in *Complex Chemistry*, Springer, Berlin **1984**, pp. 55–118.
- [32] D. Kivelson, R. Neiman, *J. Chem. Phys.* **1961**, *35*, 149.
- [33] N. M. Hosny, M. A. Hussien, F. M. Radwan, N. Nawar, *J. Mol. Struct.* **2017**, *1143*, 176.
- [34] A. Coats, J. Redfern, *Nature* **1964**, *201*, 68.
- [35] H. H. Horowitz, G. Metzger, *Anal. Chem.* **1963**, *35*, 1464.
- [36] Y. E. Sherif, N. M. Hosny, *Eur. J. Med. Chem.* **2014**, *83*, 338.
- [37] M. Hassanien, I. Gabr, M. Abdel-Rhman, A. El-Asmy, *Spectrochim. Act.* **2008**, *71*, 73.
- [38] F. Karipcin, B. Dede, Y. Caglar, D. Hür, S. Ilıcan, M. Caglar, Y. Şahin, *Opt. Commun.* **2007**, *272*, 131.
- [39] N. M. Hosny, *J. Mol. Struct.* **2009**, *923*, 98.
- [40] N. M. Hosny, *Synth. React. Inorg-Org. Met. Nano.* **2010**, *40*, 391.
- [41] N. M. Hosny, M. A. Mahmoud, M. R. E. Aly, *Synth. React. Inorg-Org. Met. Nano.* **2010**, *40*, 439.
- [42] J. Tauc, R. Grigorovici, A. Vancu, *Phys. Status Solidi (b)* **1966**, *15*, 627.
- [43] R. Pandey, S. Sahu, S. Chandra, *Handbook of Semiconductor Electrodeposition*, Marcel Dekker Inc., New York **1996**.
- [44] M. L. Fu, G. C. Guo, X. Liu, B. Liu, L.-Z. Cai, J.-S. Huang, *Inorg. Chem. Commun.* **2005**, *8*, 18.
- [45] N. M. Hosny, *Mater. Chem. Phys.* **2014**, *144*, 247.
- [46] N. M. Hosny, *Polyhedron* **2011**, *30*, 470.
- [47] N. M. Hosny, A. Dahshan, *Mater. Chem. Phys.* **2012**, *137*, 637.
- [48] N. M. Hosny, A. Dahshan, *J. Mol. Struct.* **2015**, *1085*, 78.
- [49] G. Jeffery, J. Bassett, J. Mendham, R. Denney, *Vogel's Quantitative Chemical Analysis*, Longman Scientific & Technical Longman Group UK Limited, Essex, UK **1989**.
- [50] J. Scientific, *PeakFit-Peak Separation and Analysis Software for Windows*, San Rafael CA, USA **1995**.
- [51] A. M. Abdelghany, *Spectrochim. Act.* **2013**, *100*, 120.
- [52] S. J. Azahari, M. H. Abdel Rhman, M. M. Mostafa, *Spectrochim. Act.* **2014**, *132*, 165.
- [53] T. Mosmann, *J. Immunol. Methods* **1983**, *65*, 55.
- [54] F. Denizot, R. Lang, *J. Immunol. Methods* **1986**, *89*, 271.

**How to cite this article:** Hosny NM, Mahmoud HM, Abdel-Rhman MH. Spectral, optical, and cytotoxicity studies on *N*-(2-isonicotinoylhydrazine-carbonothioyl) benzamide and its metal complexes. *Heteroatom Chem.* 2018:e21415. <https://doi.org/10.1002/hc.21415>